Original Article

Rheology Of Blood Flow With Nano Particles In An Elastic Tube

B. Sreekala1[1*], K. Maruthi Prasad[2], N. Subadra[3]

[1]Research Scholar, Department of Mathematics, School of Science, GITAM (Deemed to be University) & Department of Basic Sciences and Humanities, BVRIT HYDERABAD College of Engineering for Women, Hyderabad, India
[2]Department of Mathematics, School of Science, GITAM (Deemed to be University)
Hyderabad, India
[3]Department of Mathematics, Geethanjali College of Engineering and Technology
Hyderabad, India

[*]**Corresponding Author:** B. Sreekala

[*]Research Scholar, Department of Mathematics, School of Science, GITAM (Deemed to be University) & Department of Basic Sciences and Humanities, BVRIT HYDERABAD College of Engineering for Women, Hyderabad, India E-mail: bheemasreekala@gmail.com
Doi: 10.47750/pnr.2022.13.S05.231

Abstract

The effect of elasticity on the peristaltic flow of a micropolar fluid containing nanoparticles in a cylindrical tube is investigated using a mathematical model. The expressions for velocity and flux flow rate are determined by using Homotopy Perturbation method, under long wave length and low Reynold's number approximations. The variation of flux is calculated by Rubinow and Keller, Muzumdar methods. Different parameters' effects on velocity and flow have been discussed. For various settings, the trapping phenomenon is demonstrated. The flux increases as the elasticity parameters, micropolar parameter, thermophoresis parameter, and coupling number increase. The flux similarly reduces as the Brownian motion parameter is increased. The obtained results are same when we apply Rubinow and Keller, Muzumdar methods.

Keywords: Peristaltic flow, Elastic tube, non-Newtonian fluid, Micropolar index, Volume flow rate

INTRODUCTION

Peristalsis is a sequence of wave-like contractions of the muscles involved in the transport of food and other liquid particles in the digestive tract to various processing organs situated in the digestive system. Food digestion via oesophagus, chyme flow in the digestive tract, blood vessel movement such as capillaries, vertebral arteries, and veins, wastewater transportation from the kidney to the bladder, shift of hygienic fluids, moving of harmful fluids, transport of dangerous fluids transport in the nuclear power industry, and other applications have given peristalsis a lot of attention from contemporary scientists. Many theoretical and experimental studies on peristalsis conducted. Peristalsis was first studied by Latham [1] in 1965. Ustable peristaltic transport in curved channels was explored by Maruthi Prasad et al. [2]. Maruthi Prasad et al. [3] looked at the peristaltic motion of nanoparticles in a micropolar fluid through an inclined tube, as well as the impact of heat and mass transmission. Divya et al. [4] investigated the influence of different liquid physiognomies on the peristaltic process of a convectively heated Jeffrey fluid in a greased elastic tube. Ravikumar et al. [5] analysed heat transmission and slip belongings on MHD peristaltic movement of viscous fluid in a tapered microvessels. The effects of slip on the peristaltic transport of casson fluid in an inclined pliable tube with porous walls were studied by Gudekote & Choudhari [6].

A nanofluid is a liquid that contains nanoparticles. The fluids are colloidal nanoparticle suspensions in a base fluid that have been created. Oxides, metals, carbides, or carbon nanotubes are frequently employed as nanoparticles in nanofluids. Ethylene glycol, oil, and water are popular base fluids. Hybrid-powered engines, microelectronics, fuel cells, pharmaceutical processes, engine cooling/vehicle thermal management, chiller, heat exchanger, grinding, machining, domestic refrigerator, and boiler flue gas temperature reduction are just a few of the applications where nanofluids could be useful. Several studies have been conducted and publications have been published in the topic of nanofluids. Choi [7] was the first to investigate nanofluid technology. Nadeem and Noreen Sher Akbar [8] investigated the flow of a micropolar fluid containing nanoparticles through the small intestine. Maruthi Prasad et al. [9] investigated the peristaltic transport of a nanofluid through an inclined tube. The impact of elasticity on nanofluid peristaltic flow in a tube was investigated by Haseena et al. [10]. A computational method for MHD peristaltic transport through an inclined nanofluid symmetric channel containing porous material was provided by Abd-Alla et al. [11].

Fluids like micropolar fluids have a microstructure that belongs to the polar fluids class of fluids with a non-symmetrical strain tensor. They are essential to scientists and engineers dealing with hydrodynamic fluid problems because they physically constitute fluids comprising of arbitrarily oriented particles suspended in a viscous medium. Contributions to research in this area have been made. Maruthi Prasad et al. [12] investigated peristaltic motion of nanoparticles in a

micropolar fluid in an inclined tube with heat and mass transfer effect. The peristaltic movement of Herschel-Bulkley fluid through an unequal flexible tube was investigated by Selvi and Srinivas [13]. Ajaz Ahmad Dar [14] found peristaltic flow of a micropolar fluid with slip velocity in a tapering asymmetric channel in the presence of an inclined magnetic field and thermal radiation. Micropolar fluid in tapering stenosed arteries with porous walls has been discussed by Prasad and Yasa [15].

Fluid flow in pliable tubes is of attention because of its dynamic similarities to fluid flow in arteries, veins, and urethra, among other places. Modeling elastic distortion of hollow tubes, mechanical progress of elastic tubes used in physical therapy, cardiovascular systems to recognise the development of pathology due to vessel distortion, diagnostic and therapeutic devices such as pressurised cuffs, and prosthetic heart devices are all examples of important elastic tube applications. Many studies on elastic tubes have been conducted because of its importance. Selvi and Srinivas [16] discussed the outcome of elasticity on bingham fluid flow in a tube. Sumalatha and Sreenadh [17] investigated the poiseuille movement of a jeffrey fluid through an inclined elastic tube. The peristaltic transport of a power-law fluid in an elastic tube was studied by Selvi et al. [18]. Haseena et al. [19] investigated the influence of elasticity on nanofluid peristaltic flow in a tube.

Previous research has shown that while researching blood rheology in physiological systems, it is crucial to consider the tube's elastic nature. The current problem is to look at the effects of elasticity on a micropolar fluid flow through a tube that induces peristalsis. In this sense, blood is seen as a micropolar fluid containing nanoparticles. A technique known as Homotopy Perturbation is used to resolve the temperature profile and nanoparticle phenomena. Graphs are used to analyse the outcomes of analytic expressions for flow quantities.

MATHEMATICAL FORMULATION

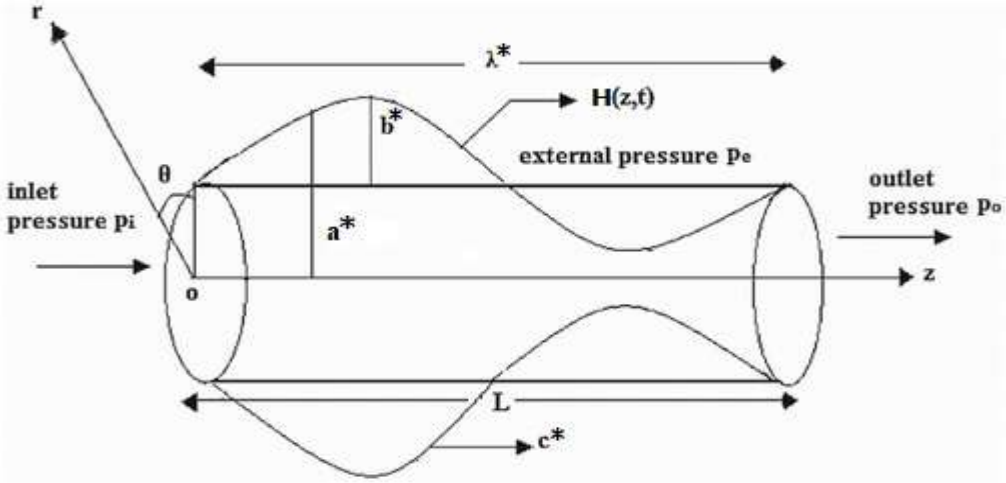

Fig. 1. Peristaltic transport of a micropolar fluid in an elastic tube

Consider the peristaltic transport of an incompressible micropolar fluid containing nano- particles in an elastic tube. The tube has a uniform cross-section with radius a^*, and sinusoidal waves with constant speed c^*, amplitude b^*, and wave length λ^* pass along its boundary. Assume that the tube is elastic at an angle α with the horizontal axis as shown in fig.1. This research took into account heat transport as well as the phenomenon of nanoparticles. At the tube's core, the symmetry requirement applies to both temperature and nanoparticle phenomena, whereas temperature $\overline{T_0}$ and nanoparticle volume fraction $\overline{C_0}$ are preserved at the tube's walls. The cylindrical polar coordinate system $(R, \theta, \bar{Z})$ is used, with the $\bar{Z}$-axis parallel to and transverse to the tube's centre line. The flow is also expected to have axial symmetry. The structure of the wall surface is defined by

$$R = H(z, t_1) = a^* + b^* \sin\frac{2\pi}{\lambda^*}(\bar{Z} - c^* t_1) \quad (1)$$

Utilizing the transformation

$$r = R, z = \bar{Z} - c^* t_1, w_z = W_z - c^*, w_r = W_r, \theta = \theta, (2)$$

Converting moving frame to fixed wave and applying non-dimensional quantities:

$$h' = \frac{H}{a^*}, r' = \frac{r}{a^*}, z' = \frac{z}{\lambda^*}, P' = \frac{a^{*2}P}{\lambda^* \mu_{c_1} c^*}, w_r' = \frac{\lambda^* w_r}{c^* a^*}, w_z' = \frac{w_z}{c^*}, v_\theta' = \frac{v_\theta}{a^{*2}}, t' = \frac{c^* t_1}{\lambda^*},$$

$$j' = \frac{j}{a^{*2}}, \theta = \frac{T - \overline{T_0}}{\overline{T_0}}, \delta = \frac{a^*}{\lambda^*}, R_e = \frac{2\rho c^* a^*}{\mu}, \sigma = \frac{\bar{C_1} - \overline{C_0}}{\overline{C_0}}, N_b = \frac{(\rho C_1)_P D_{\bar{B}} \overline{C_0}}{(\rho C_1)_f},$$

$$N_t = \frac{(\rho C_1)_P D_T \overline{T_0}}{(\rho C_1)_f \beta}, G_r = \frac{g\omega a^{*3} \overline{T_0}}{\gamma^2}, B_r = \frac{g\omega a^{*3} \overline{C_0}}{\gamma^2}$$

Under the long wave length approximation and low Reynold's number, the equations of an incompressible microploar fluid containing nanoparticles are defined [12] as

$$\frac{\partial p}{\partial r} = 0 \qquad (3)$$

$$(1-N)\frac{\partial p}{\partial z} = \frac{N}{r}\frac{\partial}{\partial r}(rv_\theta) + \frac{\partial^2 w}{\partial r^2} + \frac{1}{r}\frac{\partial w}{\partial r} + (1-N)(G_r\theta + B_r\sigma) \quad (4)$$

$$2v_\theta + \frac{\partial w}{\partial r} - \frac{2-N}{m^2}\frac{\partial}{\partial r}\left(\frac{1}{r}\frac{\partial}{\partial r}(rv_\theta)\right) = 0 \quad (5)$$

$$0 = \frac{1}{r}\frac{\partial}{\partial r}\left(r\frac{\partial\theta}{\partial r}\right) + N_b\left(\frac{\partial\sigma}{\partial r}\right)\left(\frac{\partial\theta}{\partial r}\right) + N_t\left(\frac{\partial\theta}{\partial r}\right)^2 \quad (6)$$

$$0 = \frac{1}{r}\frac{\partial}{\partial r}\left(r\frac{\partial\sigma}{\partial r}\right) + \frac{N_t}{N_b}\left(\frac{1}{r}\frac{\partial}{\partial r}\left(r\frac{\partial\theta}{\partial r}\right)\right) \quad (7)$$

The velocity in the axial direction is denoted by w. Here N is coupling number, m is the micropolar parameter, Brownian motion parameter, Thermophoresis parameter, Local temperature Grashof number, and Local nanoparticle Grashof number are N_b , N_t , G_r and B_r respectively.

The following are non-dimensional boundary conditions:

$$\begin{cases} \frac{\partial w}{\partial r} = 0, \ \ \frac{\partial\theta}{\partial r} = 0, \ \ \frac{\partial\sigma}{\partial r} = 0 & at \quad r = 0 \\ w = -1, \theta = 0, \sigma = 0, v_\theta = 0 & at \quad r = h(z) = 1 + \varepsilon \sin 2\pi z \\ v_\theta \ is \ finite, \ \ w \ is \ finite & at \quad r = 0 \end{cases} \qquad (8)$$

The amplitude ratio ε is equal to $\frac{a^*}{b^*}$

Solution

The Homotopy Perturbation technique (He JH, [20]) is used to solve equations (6) and (7) are as follows:

$$H(q,\theta) = L(\theta) - L(\theta_{10}) + qL(\theta_{10}) + q\left[N_b\frac{\partial\sigma}{\partial r}\frac{\partial\theta}{\partial r} + N_t\left(\frac{\partial\theta}{\partial r}\right)^2\right] (9)$$

$$H(q,\sigma) = L(\sigma) - L(\sigma_{10}) + qL(\sigma_{10}) + q\left[\frac{N_t}{N_b}\frac{1}{r}\frac{\partial}{\partial r}\left(r\frac{\partial\theta}{\partial r}\right)\right] (10)$$

For the sake of simplicity, $L = \frac{1}{r}\frac{\partial}{\partial r}\left(r\frac{\partial}{\partial r}\right)$ is used as a linear operator.

$$\theta_{10}(r,z) = \left(\frac{r^2-h^2}{4}\right), \sigma_{10}(r,z) = -\left(\frac{r^2-h^2}{4}\right) \quad (11)$$

are referred to as initial estimates that satisfy the boundary conditions.

Define

$$\theta(r,z) = \theta_0 + q\theta_1 + q^2\theta_2 + \ldots \quad (12)$$

$$\sigma(r,z) = \sigma_0 + q\sigma_1 + q^2\sigma_2 + \ldots \quad (13)$$

For the most part, the series (12) and (13) are convergent. The convergent rate is affected by the nonlinear component of the equation.

Using the same method as He JH, [20], for q=1, the temperature and nanoparticle phenomena solution is as follows:

$$\theta(r,z) = N_b(N_b - N_t)\left(\frac{r^6-h^6}{1152}\right) - N_t(N_b - N_t)\left(\frac{r^6-h^6}{576}\right) - (N_b - 2N_t)\left(\frac{r^4-h^4}{64}\right) \quad (14)$$

$$\sigma(r,z) = -\frac{N_t}{N_b}(N_b - N_t)\left(\frac{r^4-h^4}{64}\right) \quad (15)$$

Solving for v_θ, we get the general solution by Substituting equations (12) and (13) in equation (4).

$$v_\theta = c_2(z)I_1(mr) + c_3(z)k_1(mr) + \frac{N-1}{2-N}\frac{r}{2}\frac{dp}{dz} + \frac{1-N}{2-N}G_rN_b(N_b - N_t)\left[\frac{rh^6}{2304} + \frac{r}{m^6} + \frac{r^3}{8m^4} + \frac{r^5}{192m^2} + \frac{r^7}{9216}\right] +$$
$$\frac{1-N}{2-N}G_rN_t(N_b - N_t)\left[\frac{rh^6}{1152} - \frac{2r}{m^6} - \frac{r^3}{4m^4} - \frac{r^5}{96m^2} - \frac{r^7}{4608}\right] + \frac{1-N}{2-N}G_r(N_b - 2N_t)\left[\frac{rh^4}{128} - \frac{19}{48}\frac{r}{m^4} - \frac{19}{384}\frac{r^2}{m^2} - \frac{r^5}{384}\right] +$$
$$\frac{1-N}{2-N}B_r\frac{N_t}{N_b}(N_b - N_t)\left[\frac{rh^4}{128} - \frac{19}{48}\frac{r}{m^4} - \frac{19}{384}\frac{r^2}{m^2} - \frac{r^5}{384}\right] (16)$$

Where $I_1(mr)$ and $k_1(mr)$ are first and second order modified Bessel functions respectively.

Finally, solving for w by substituting the value of v_θ and applying the boundary conditions (8)

$$w = -Nc_2(z)\frac{I_0(mr)}{m} + \frac{1-\mathrm{N}}{2-\mathrm{N}}\frac{\mathrm{r}^2}{2}\frac{\mathrm{dp}}{\mathrm{dz}} - (1-\mathrm{N})\mathrm{G_r}\mathrm{N_b}(\mathrm{N_b} - \mathrm{N_t})\left[\frac{\mathrm{N}}{2-\mathrm{N}}\left(\frac{\mathrm{r}^2\mathrm{h}^6}{4608} + \frac{\mathrm{r}^2}{2\mathrm{m}^6} + \frac{\mathrm{r}^4}{32\mathrm{m}^4} + \frac{\mathrm{r}^6}{1152\mathrm{m}^2} + \frac{\mathrm{r}^8}{73728}\right) + \frac{\mathrm{r}^8}{73728} - \frac{\mathrm{r}^2\mathrm{h}^6}{4608}\right] -$$
$$(1-\mathrm{N})\mathrm{G_r}\mathrm{N_t}(\mathrm{N_b} - \mathrm{N_t})\left[\frac{\mathrm{N}}{2-\mathrm{N}}\left(\frac{\mathrm{r}^2\mathrm{h}^6}{2304} - \frac{\mathrm{r}^2}{\mathrm{m}^6} - \frac{\mathrm{r}^4}{16\mathrm{m}^4} - \frac{\mathrm{r}^6}{576\mathrm{m}^2} - \frac{\mathrm{r}^8}{36864}\right) - \frac{\mathrm{r}^8}{36864} + \frac{\mathrm{r}^2\mathrm{h}^6}{2304}\right] - (1-\mathrm{N})\mathrm{G_r}(\mathrm{N_b} -$$
$$2\mathrm{N_t})\left[\frac{\mathrm{N}}{2-\mathrm{N}}\left(\frac{\mathrm{r}^2\mathrm{h}^4}{256} - \frac{19\mathrm{r}^2}{96\mathrm{m}^4} - \frac{19\mathrm{r}^3}{1152\mathrm{m}^2} - \frac{\mathrm{r}^6}{2304}\right) - \frac{\mathrm{r}^6}{2304} + \frac{\mathrm{r}^2\mathrm{h}^4}{256}\right] - (1-\mathrm{N})\mathrm{B_r}\frac{\mathrm{N_t}}{\mathrm{N_b}}(\mathrm{N_b} - \mathrm{N_t})\left[\frac{\mathrm{N}}{2-\mathrm{N}}\left(\frac{\mathrm{r}^2\mathrm{h}^4}{256} - \frac{19\mathrm{r}^2}{96\mathrm{m}^4} - \frac{19\mathrm{r}^3}{1152\mathrm{m}^2} - \frac{\mathrm{r}^6}{2304}\right) -$$
$$\frac{\mathrm{r}^6}{2304} + \frac{\mathrm{r}^2\mathrm{h}^4}{256}\right] + c_4 \ (17)$$

Where c_2,c_3 and c_4 are arbitrary constants that can be found by applying boundary conditions on w,

The dimension less flux is

$$Q = \int_0^h rw\,dr \qquad (18)$$

Substituting equation (17) in equation (18), we get

$$Q = P\left[\frac{N}{m}\frac{1-N}{2-N}h^2 + \frac{1-N}{2-N}\frac{h^4}{4} - \frac{N}{m}\frac{1-N}{2-N}\frac{I_0(mh)}{I_1(mh)}\frac{h^3}{2}\right] + F \ (19)$$

Where $F = -h^2 + \frac{N}{m}\frac{1-N}{2-N}\frac{I_0(mh)}{I_1(mh)}Ah^2 - \frac{N}{m}\frac{1-N}{2-N}2hA + Bh^2 - (1-\mathrm{N})\mathrm{G_r}\mathrm{N_b}(\mathrm{N_b}-\mathrm{N_t})\left[\frac{2\mathrm{N}}{2-\mathrm{N}}\left(\frac{41\mathrm{h}^{10}}{18432} + \frac{\mathrm{h}^8}{9216\mathrm{m}^2} + \frac{h^6}{192\mathrm{m}^4} + \frac{\mathrm{h}^4}{8m^6}\right) - \frac{13\mathrm{h}^{10}}{245760}\right] - (1-\mathrm{N})\mathrm{G_r}\mathrm{N_t}(\mathrm{N_b}-\mathrm{N_t})\left[\frac{2\mathrm{N}}{2-\mathrm{N}}\left(\frac{13\mathrm{h}^{10}}{122880} - \frac{\mathrm{h}^8}{4608\mathrm{m}^2} - \frac{h^6}{96\mathrm{m}^4} - \frac{\mathrm{h}^4}{4m^6}\right) + \frac{13\mathrm{h}^{10}}{122880}\right] - (1-\mathrm{N})\mathrm{G_r}(\mathrm{N_b} - 2\mathrm{N_t})\left[\frac{2\mathrm{N}}{2-\mathrm{N}}\left(\frac{17\mathrm{h}^8}{18432} - \frac{19h^5}{5760m^2} - \frac{19\mathrm{h}^4}{18432m^4}\right) + \frac{17h^8}{18432}\right] - (1-\mathrm{N})B_\mathrm{r}\frac{N_t}{N_b}(\mathrm{N_b}-\mathrm{N_t})\left[\frac{2\mathrm{N}}{2-\mathrm{N}}\left(\frac{17\mathrm{h}^8}{18432} - \frac{19h^5}{5760m^2} - \frac{19\mathrm{h}^4}{18432m^4}\right) + \frac{17h^8}{18432}\right]$

And $P = -\frac{dp}{dz}$

Where $A = -G_rN_b(N_b-N_t)\left[\frac{5h^7}{9216} + \frac{h^5}{192m^2} + \frac{h^3}{8m^4} + \frac{h}{m^6}\right] - G_rN_t(N_b-N_t)\left[\frac{h^7}{1536} - \frac{h^5}{96m^2} - \frac{h^3}{4m^4} - \frac{2h}{m^6}\right] - G_r(N_b-2N_t)\left[\frac{h^5}{192} - \frac{19}{384}\frac{h^2}{m^2} - \frac{19}{48}\frac{h}{m^4}\right] - B_r\frac{N_t}{N_b}(N_b-N_t)\left[\frac{h^5}{192} - \frac{19}{384}\frac{h^2}{m^2} - \frac{19}{48}\frac{h}{m^4}\right]$

and

$B = (1-N)G_rN_b(N_b-N_t)\left[\frac{N}{2-N}\left(\frac{17h^8}{73728} + \frac{h^6}{1152m^2} + \frac{h^4}{32m^4} + \frac{h^2}{2m^6}\right) - \frac{5h^8}{24576}\right] + (1-N)G_rN_t(N_b-N_t)\left[\frac{N}{2-N}\left(\frac{5h^8}{12288} - \frac{h^6}{576m^2} - \frac{h^4}{16m^4} - \frac{h^2}{m^6}\right) + \frac{5h^8}{12288}\right] + (1-N)G_r(N_b-2N_t)\left[\frac{N}{2-N}\left(\frac{h^6}{288} - \frac{19h^3}{1152m^2} - \frac{19h^2}{96m^4}\right) + \frac{h^6}{288}\right] + (1-N)B_r\frac{N_t}{N_b}(N_b - N_t)\left[\frac{N}{2-N}\left(\frac{h^6}{288} - \frac{19h^3}{1152m^2} - \frac{19h^2}{96m^4}\right) + \frac{h^6}{288}\right]$

THEORETICAL DETERMINATION OF FLUX

The flux of micropolar fluid via an elastic tube is calculated using Rubinow and Keller [22]. Let p_0 represent the external pressure and p_1 and p_2 represent the fluid pressures at the entrance and exit, respectively. The pressure at the entrance, p_1, is expected to be higher than the pressure at the exit, p_2. The tube wall can expand or shrink as the pressure within and outside the tube changes. The conductivity of the tube at z is affected by pressure variance. As a result, the conductivity function $\sigma = \sigma[p(z) - p_0]$ is equal to $(p(z) - p_0)$. The flow Q and the pressure gradient are also linked in this expression.

$$Q = \sigma(p-p_0)(P+F) \quad (20)$$

Where $\sigma(p-p_0) = \frac{N}{m}\frac{1-N}{2-N}h^2 + \frac{1-N}{2-N}\frac{h^2}{4} - \frac{N}{m}\frac{1-N}{2-N}\frac{I_0(mh)}{I_1(mh)}\frac{h^3}{2}$

Using the inlet condition and from $z = 0$, integrating equation (20) with respect to z $p(0) = p_1$, we obtain

$$Q_z = \int_{p(z)-p_0}^{p_1-p_0}\sigma(p')\,dp' + \int_0^z\left[\frac{N}{m}\frac{1-N}{2-N}h^2 + \frac{1-N}{2-N}\frac{h^2}{4} - \frac{N}{m}\frac{1-N}{2-N}\frac{I_0(mh)}{I_1(mh)}\frac{h^3}{2}\right]dz \quad (21)$$

$p' = p(z) - p_0$ in this case. Equation (21) gives $p(z)$, In terms of Q and z. By substituting $z = 1$ and $p(1) = p_2$ into the equation (21), we get Q

$$Q_z = \int_{p(1)-p_0}^{p_1-p_0}\sigma(p')\,dp' + \int_0^z\left[\frac{N}{m}\frac{1-N}{2-N}h^2 + \frac{1-N}{2-N}\frac{h^2}{4} - \frac{N}{m}\frac{1-N}{2-N}\frac{I_0(mh)}{I_1(mh)}\frac{h^3}{2}\right]dz \quad (22)$$

In this instance, where $h = h(p-p_0)$.

On the other hand, equation (22) can be written as

$$Q = \int_{p_2-p_0}^{p_1-p_0}\left[\frac{N}{m}\frac{1-N}{2-N}h^2 + \frac{1-N}{2-N}\frac{h^2}{4} - \frac{N}{m}\frac{1-N}{2-N}\frac{I_0(mh)}{I_1(mh)}\frac{h^3}{2}\right]dp' + F\left[\frac{N}{m}\frac{1-N}{2-N}h^2 + \frac{1-N}{2-N}\frac{h^2}{4} - \frac{N}{m}\frac{1-N}{2-N}\frac{I_0(mh)}{I_1(mh)}\frac{h^3}{2}\right] \quad (23)$$

The equilibrium condition determines $h(p-p_0)$, If the strain or tension $T(h)$ in the tube wall is known as a function of h.

$$\frac{T(h)}{h} = p - p_0 \quad (24)$$

METHOD OF RUBINOW AND KELLER

The fixed pressure-volume relationship of a 4cm piece of human external artery is transformed to a tension against length curve, which is then applied to arterial flow. Rubinow and Keller [22] calculated the subsequent equation using the least-squares approach.

$$T(h) = t_1(h-1) + t_2(h-1)^5 \quad (25)$$

When we use (25) in place of (24), we get

$$\mathrm{d}p' = \left[\frac{t_1}{h^2} + t_2\left(4h^3 - 15h^2 + 20h - 10 + \frac{1}{h^2}\right)\right]dh \quad (26)$$

where $t_1 = 13$ and $t_2 = 300$

Equation (23) can be written as, using equation (26)

$$Q = \int_{p_2-p_0}^{p_1-p_0}\left[\frac{N}{m}\frac{1-N}{2-N}h^2 + \frac{1-N}{2-N}\frac{h^2}{4} - \frac{N}{m}\frac{1-N}{2-N}\frac{I_0(mh)}{I_1(mh)}\frac{h^3}{2}\right]\left[\frac{t_1}{h^2} + t_2\left(4h^3 - 15h^2 + 20h - 10 + \frac{1}{h^2}\right)\right]dh + F(h(p_2-p_0)^4) \quad (27)$$

Flux is simplified even further

$$Q = \frac{1}{8}\left[\left(g(h_1) - g(h_2)\right) + Fh_2^4\right]$$

Where $g(h) = t_1\left[\frac{N}{m}\frac{1-N}{2-N}h + \frac{1-N}{2-N}\frac{h^3}{12} - \frac{N}{m}\frac{1-N}{2-N}\frac{I_0(mh)}{I_1(mh)}\frac{h^3}{8}\right] + t_2\left[\frac{N}{m}\frac{1-N}{2-N}\left(\frac{2h^6}{3} - 3h^5 + 5h^4 - \frac{10h^3}{3} + h\right) + \frac{1-N}{2-N}\left(\frac{h^8}{8} - \frac{15h^7}{28} + \frac{5h^6}{6} - \frac{h^5}{2} + \frac{h^3}{12}\right) - \frac{N}{m}\frac{1-N}{2-N}\frac{I_0(mh)}{I_1(mh)}\left(\frac{2h^7}{7} - \frac{15h^6}{12} + h^5 - \frac{5h^4}{4} + \frac{h^2}{4}\right)\right]$

$h_1 = h(p_1 - p_0)$

$$h_2 = h(p_2 - p_0) \quad (28)$$

METHOD OF MAZUMDAR

The tension relationship can be written as follows, according to Mazumdar [21]

$$T(h) = A(e^{kh} - e^k) \quad (29)$$

By substituting Eq. (29) in Eq. (24) for $A = 0.007435$ and $k = 5.2625$, we get

$$p - p_0 = A\left[\frac{e^{Kh}}{h} - \frac{e^K}{h}\right]$$

$$dp' = A\left[e^{Kh}\left(\frac{K}{h} - \frac{1}{h^2}\right) + \frac{e^K}{h^2}\right]dh \quad (30)$$

We get the flux by putting Eq. (30) into Eq. (23)

$$Q = \int_{p_2-p_0}^{p_1-p_0}\left[\frac{N}{m}\frac{1-N}{2-N}h^2 + \frac{1-N}{2-N}\frac{h^2}{4} - \frac{N}{m}\frac{1-N}{2-N}\frac{I_0(mh)}{I_1(mh)}\frac{h^3}{2}\right]A\left[e^{Kh}\left(\frac{K}{h} - \frac{1}{h^2}\right) + \frac{e^K}{h^2}\right]dh + F(h(p_2 - p_0)^4)$$

Where $h = h(p - p_0)$

$$Q = \left[\left(g(h_1) - g(h_2)\right)\right] + Fh_2^4 \quad (31)$$

Where $g(h) = \frac{N}{m}\frac{1-N}{2-N}\left[\frac{e^{kh}}{k^2}(k^2h - 2k) + he^k\right] + \frac{1-N}{2-N}\frac{1}{4}\left[\frac{e^{kh}}{k^4}(k^4h^3 - 4k^3h^2 + 4k^2h - 8k) + e^k\frac{h^3}{3}\right] - \frac{N}{m}\frac{1-N}{2-N}\frac{I_0(mh)}{I_1(mh)}\frac{1}{2}\left[\frac{e^{kh}}{k^3}(k^3h^2 - 3k^2h + 3k) + e^k\frac{h^2}{2}\right]$

RESULTS AND DISCUSSIONS

The flow pattern of peristaltic blood transport in an elastic tube was investigated in this research. Blood is regarded as a micropolar fluid in this experiment. Graphs are used to examine the impacts of several physiological characteristics on flow rate, such as micropolar parameter (m), Brownian motion parameter (N_b), Thermophoresis parameter (N_t), Local temperature Grashof number (G_r), and local nanoparticle Grashof number (B_r). Mathematica 9.1 was used to create the graphs.

Figures 2-9 show the influence of various parameters on the flux. The flow is computed using Rubinow and Keller method in this case.

The flux increases as the radius of the tube grows, as seen in fig. 2-3. It was also observed that as the elastic parameters t_1 and t_2 increase, the volume flow rate increases.

The flux grows as the radius of the tube increases, as seen in fig.4-5. This is due to the Brownian motion parameter, which states that as the radius of the tube increases, so does the collision between the molecules, causing the flux to increase. It's worth noting that this rise is significant for values of the tube's radius greater than 2.5. The flux increases as the thermophoresis parameter is increased (Fig.4).

As can be seen in figures 6-8, the flux increases as the radius grows. The volume flow rate increases with local temperature Grashof number (G_r), coupling number (N), and micro polar parameter (m), according to the figures.

From the fig. 9 it is noticed that, the flux decreases as the local nanoparticle Grashof number (B_r) increases, but this is only noticeable after the tube radius reaches 1.4.

FLUX CHARACTERISTICS

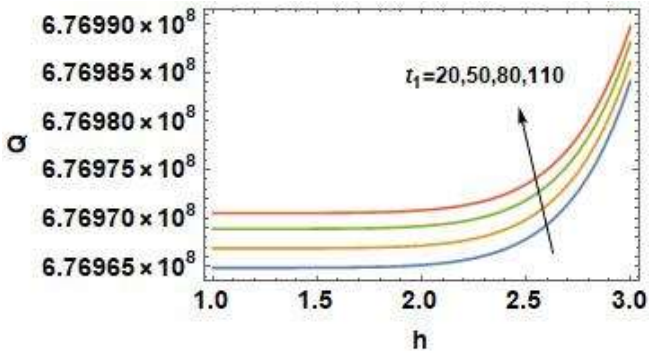

Fig. 2. Flux Q versus radius h with various values of the elastic parameter t_1 when $t_2 = 100,\ N_b = 12,\ N_t = 20,\ G_r = 8,\ B_r = 20,\ N = 0.8,\ m = 2.5$ (Rubinow and Keller)

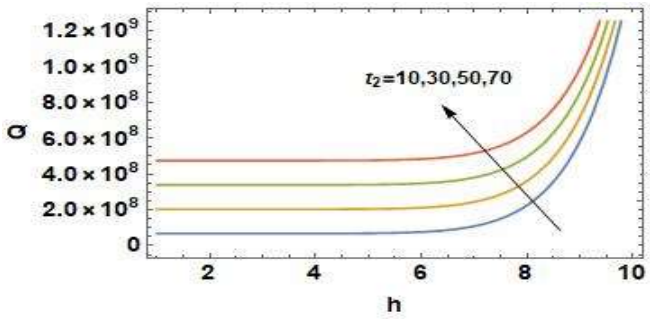

Fig. 3. Flux Q versus radius h with various values of the elastic parameter t_2 when $t_1 = 50, N_b = 12, N_t = 20, G_r = 8, B_r = 20, N = 0.8, m = 2.5$ (Rubinow and Keller)

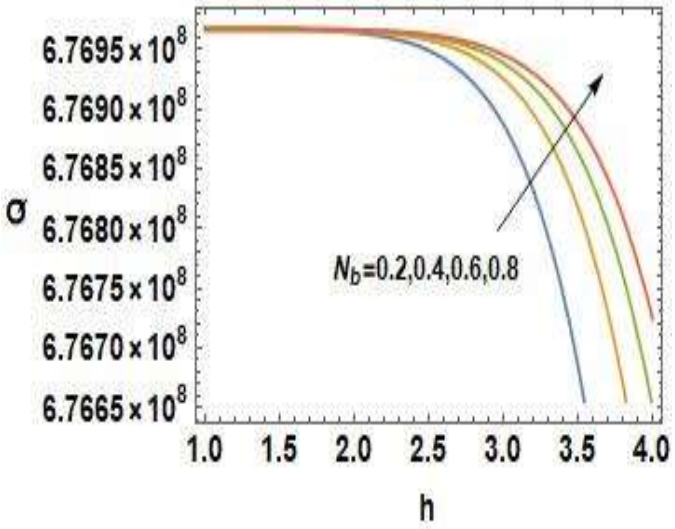

Fig. 4. Flux Q versus radius h with various values of the Brownian motion parameter N_b when $t_1 = 50, t_2 = 100, N_t = 15, G_r = 6, B_r = 15, N = 0.8, m = 2.5$ (Rubinow and Keller)

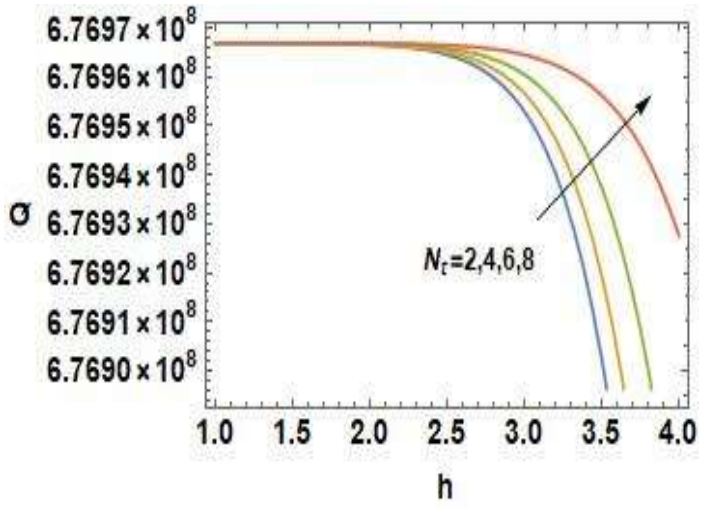

Fig. 5. Flux Q versus radius h with various values of the Thermophoresis parameter N_t when $t_1 = 50, t_2 = 100, N_b = 9, G_r = 6, B_r = 15, N = 0.8, m = 2.5$ (Rubinow and Keller)

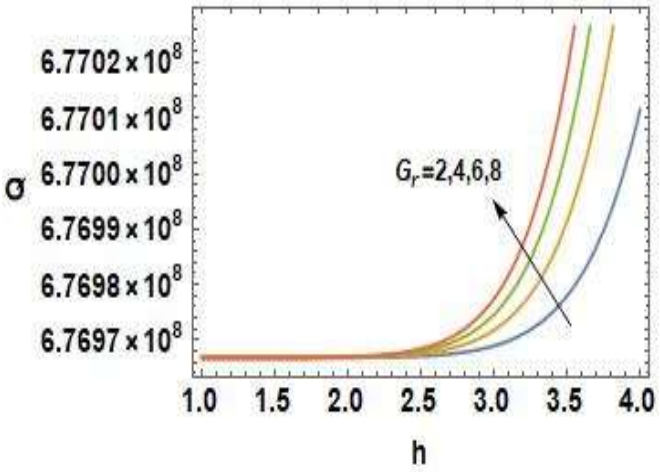

Fig. 6. Flux Q versus radius h with various values of the local temperature Grashof number G_r when $t_1 = 50, t_2 = 100, N_b = 9, G_r = 6, B_r = 15, N = 0.8, m = 2.5$ (Rubinow and Keller)

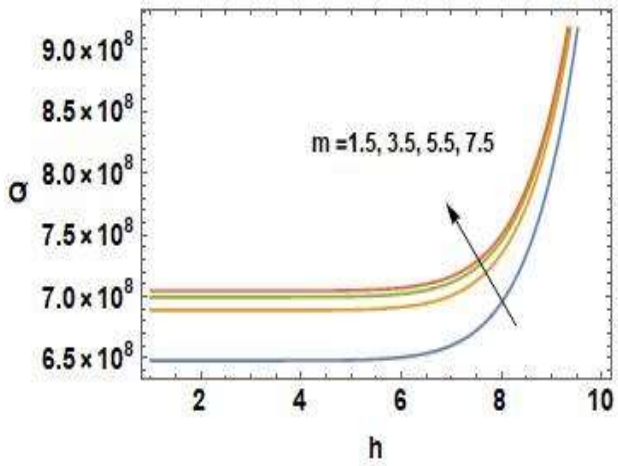

Fig. 7. Flux Q versus radius h with various values of the micropolar parameter m when $t_1 = 50, t_2 = 100, N_b = 6,\ N_t = 10, G_r = 4, B_r = 10, N = 0.8$ (Rubinow and Keller)

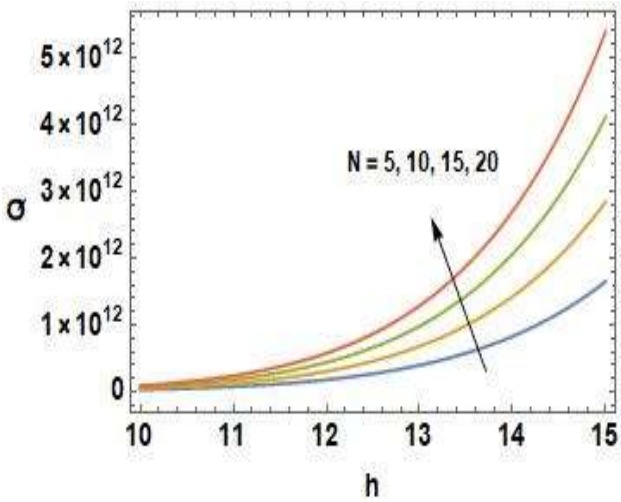

Fig. 8. Flux Q versus radius h with various values of the coupling number N when $t_1 = 50, t_2 = 100, N_b = 6,\ N_t = 10, G_r = 4, B_r = 10, m = 2.5$ (Rubinow and Keller)

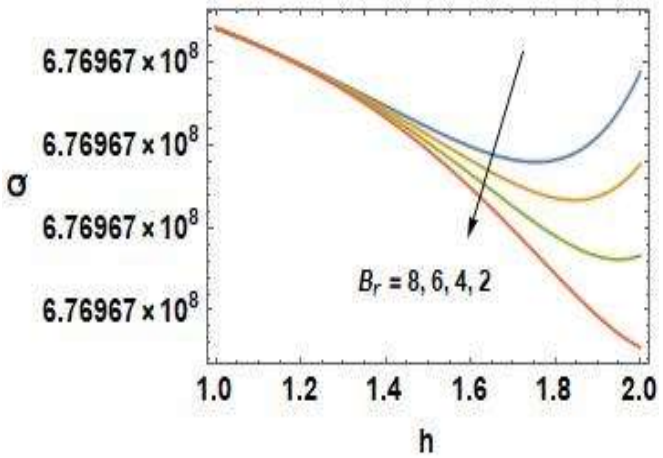

Fig. 9. Flux Q versus radius h with various values of the local nanoparticle Grashof number B_r when $t_1 = 50, t_2 = 100, N_b = 3, N_t = 5, G_r = 2, N = 0.8, m = 2.5$ (Rubinow and Keller)

The Rubinow Keller technique exhibits the same behaviour as fig.10-17.
The impacts of various parameters on the flux determined using the Mazumdar approach is shown in figures 10–17.
Fig.10-16 it is indicated that the flux rises with radius, elastic parameters K and A [for numerical computation using the values of A=0.007435 and K=5.2625], Brownian motion parameter (N_b) , Thermophoresis parameter (N_t), Local temperature Grashof number (G_r), local nanoparticle Grashof number (B_r), micro polar parameter (m) and coupling number (N).
The volume flow rate decreases as the radius and local nanoparticle Grashof number (B_r) rise, as depicted in fig.17.

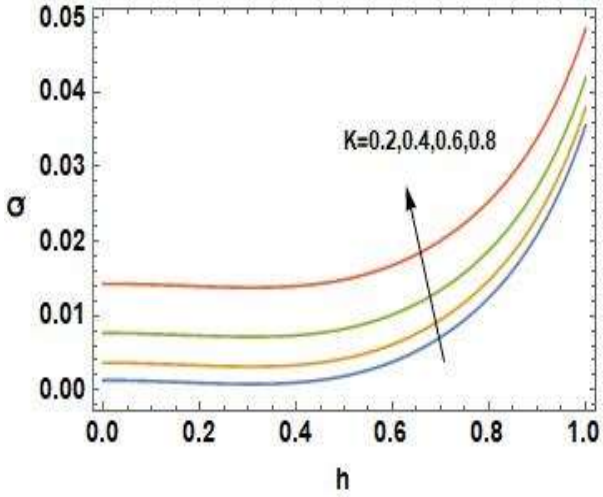

Fig. 10. Flux Q versus radius h with various values of the elastic parameter K when $A = 0.0074,\ N_b = 12,\ N_t = 20,\ G_r = 8,\ B_r = 20,\ N = 0.8,\ m = 2.5$ (Mazumdar method)

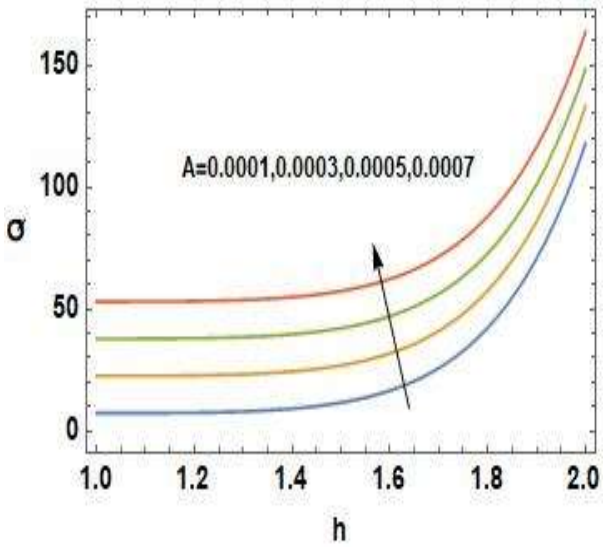

Fig. 11. Flux Q versus radius h with various values of the elastic parameter A when $K = 5.26,\ N_b = 9,\ N_t = 15,\ G_r = 6,\ B_r = 15,\ N = 0.8,\ m = 2.5$ (Mazumdar method)

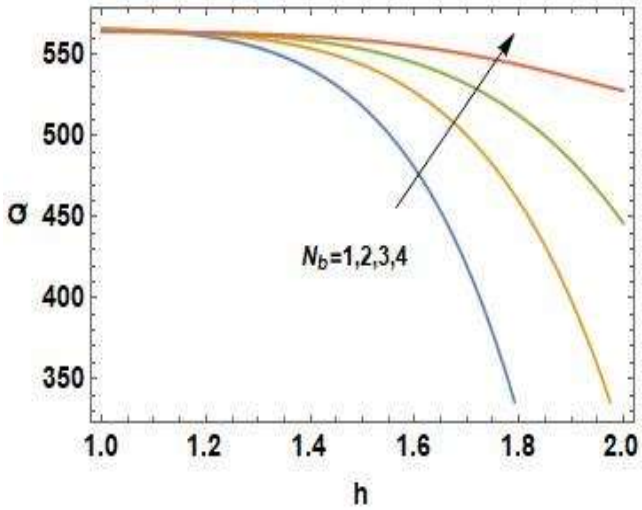

Fig. 12. Flux Q versus radius h with various values of the Brownian motion parameter N_b when $K = 5.26, A = 0.0074, N_t = 15, G_r = 6, B_r = 15, N = 0.8, m = 2.5$ (Mazumdar method)

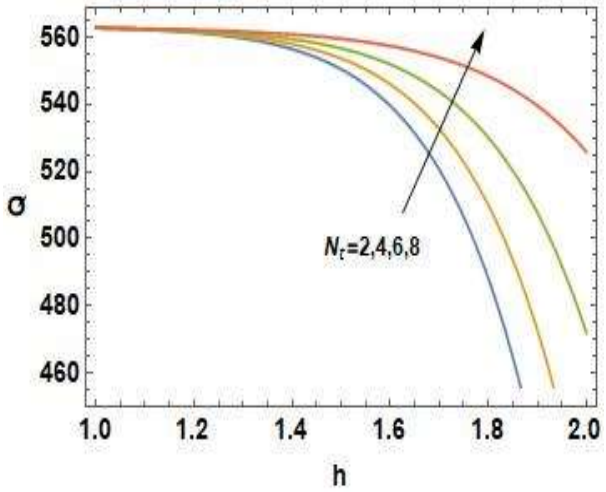

Fig. 13. Flux Q versus radius h with various values of the Thermophoresis parameter N_t when $K = 5.26, A = 0.0074, N_b = 9, G_r = 6, B_r = 15, N = 0.8, m = 2.5$ (Mazumdar method)

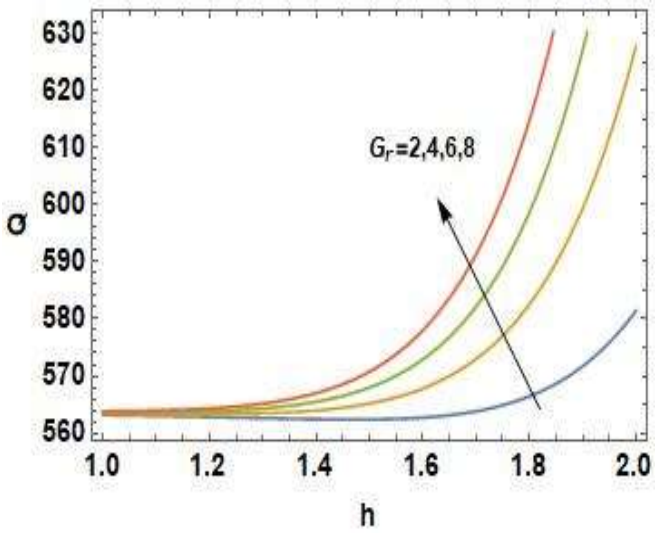

Fig. 14. Flux Q versus radius h with various values of the local temperature Grashof number G_r when $K = 5.26,\ A = 0.0074,\ N_b = 9, N_t = 15,\ B_r = 15,\ N = 0.8,\ m = 2.5$ (Mazumdar method)

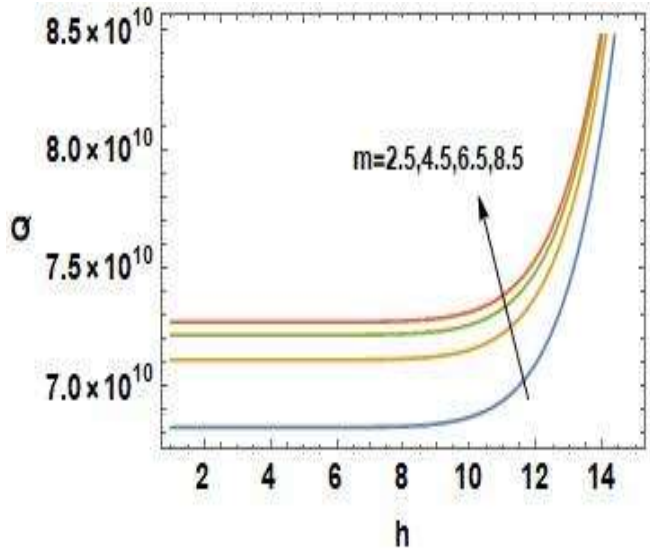

Fig. 15. Flux Q versus radius h with various values of the micropolar parameter m when $K = 5.26,\ A = 0.0074, N_b = 6,$ $N_t = 10, G_r = 4, B_r = 10, N = 0.8$ (Mazumdar method)

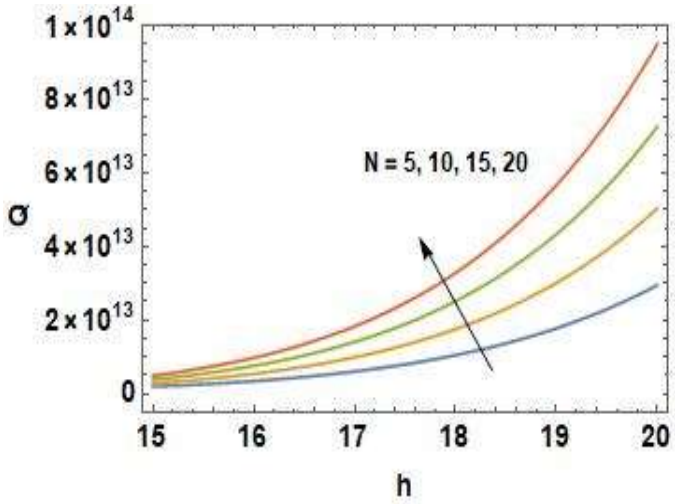

Fig. 16. Flux Q versus radius h with various values of the coupling number N when $K = 5.26,\ A = 0.0074, N_b = 6,$ $N_t = 10, G_r = 4, B_r = 10, m = 2.5$ (Mazumdar method)

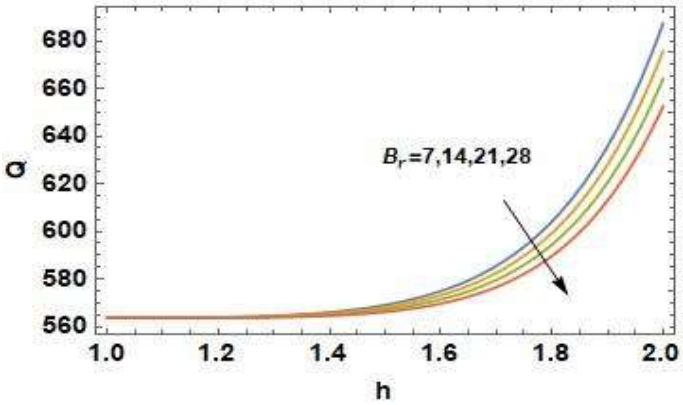

Fig. 17. Flux Q versus radius h with various values of the local nanoparticle Grashof number B_r when $K = 5.26,\ A = 0.0074, N_b = 9, N_t = 15, G_r = 6, N = 0.8, m = 2.5$ (Mazumdar method)

STREAMLINE PATTERNS

Trapping is a remarkable fluid movement phenomenon. In other cases, the wave frame's streamlines swell to capture a bolus that flows with the wave speed as an inlet. Trapping is the process of a closed streamline producing an internally circulating bolus. The wave pattern moves the bolus, which is defined by way of a flowing fluid surrounded by curved streamlines in the wave frame. The streamlining patterns for various parameters are depicted in figures 18-21. When the

values of N_b and B_r increase, the trapping boluses grow, whereas when the values of N_t and G_r increase, the trapping boluses diminish.

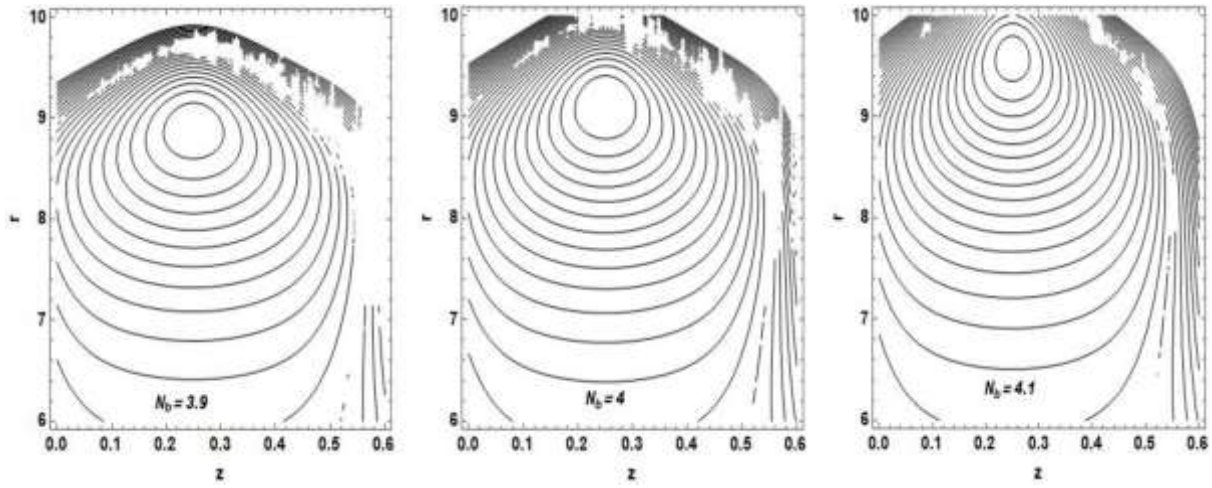

Fig. 18. Streamlines for $N_b = 3.9,\ 4,\ 4.1$

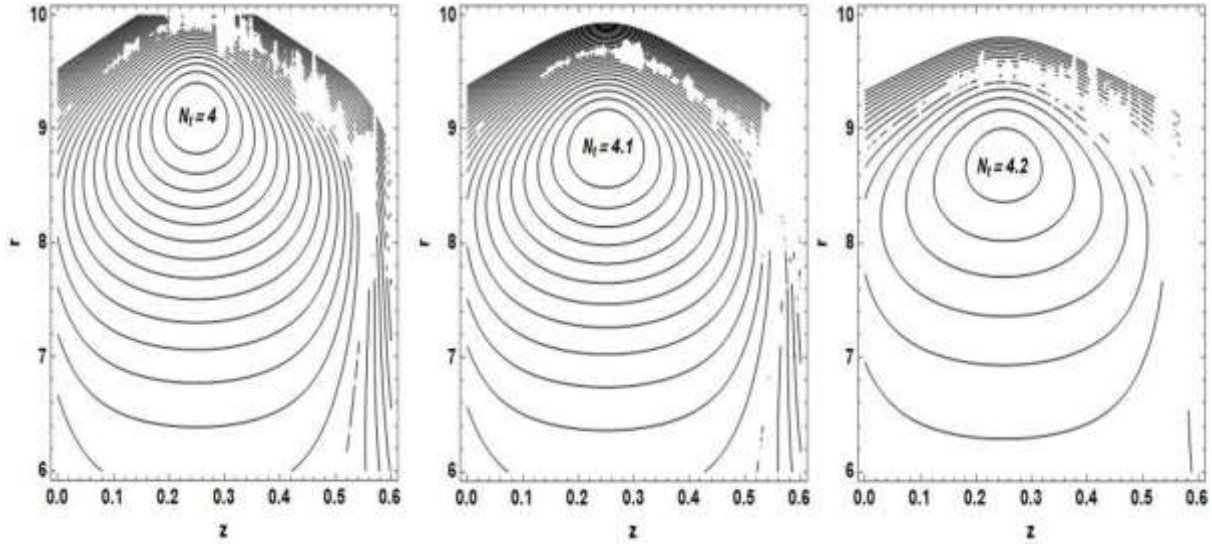

Fig. 19. Streamlines for $N_t = \ 4,\ 4.1, 4.2$

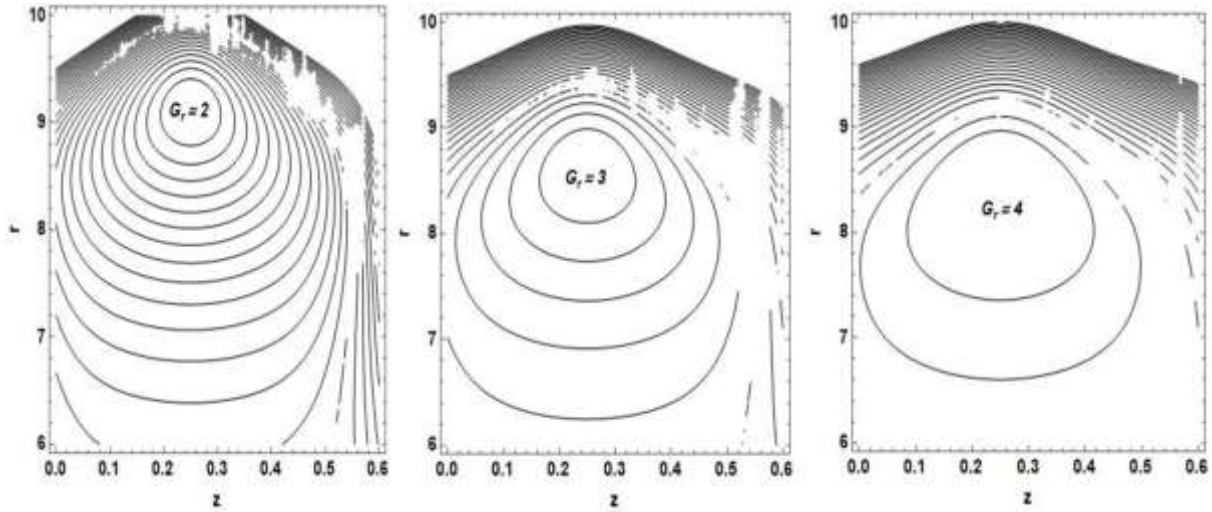

Fig. 20. Streamlines for $G_r = \ 2,\ 3,\ 4$

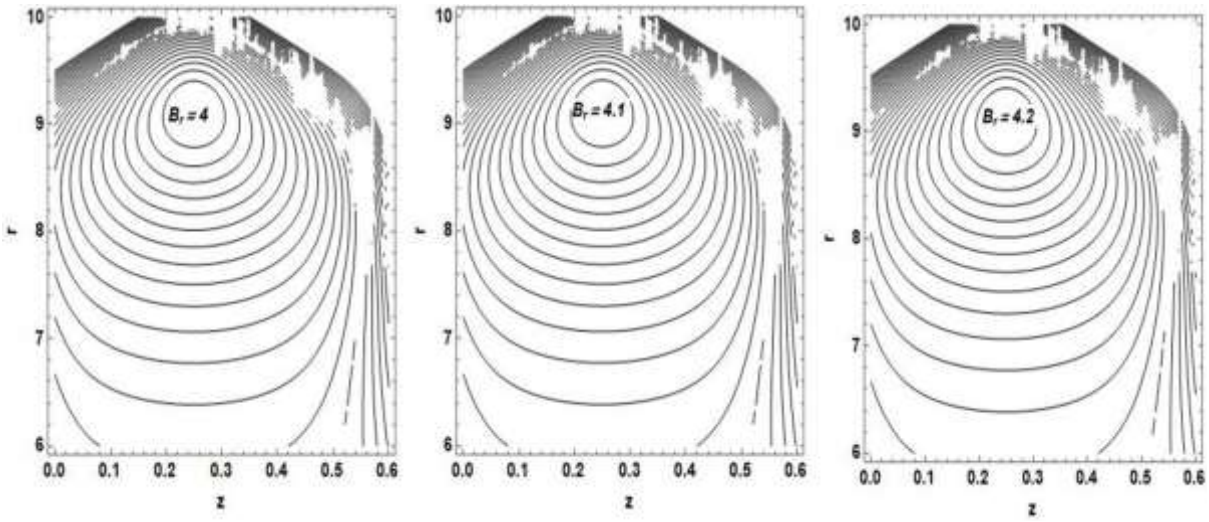

Fig. 21. Streamlines for $B_r = 4,\ 4.1,\ 4.2$

VELOCITY PROFILES

Figures 22–23 show velocity profiles with radius of the elastic tube for various values of N_b, N_t, G_r, and B_r. It is seen that, the velocity rises with increasing values of Brownian motion parameter $[N_b]$, Thermophoresis parameter $[N_t]$, Local temperature Grashof number $[G_r]$and Local nanoparticle Grashof number $[B_r]$.

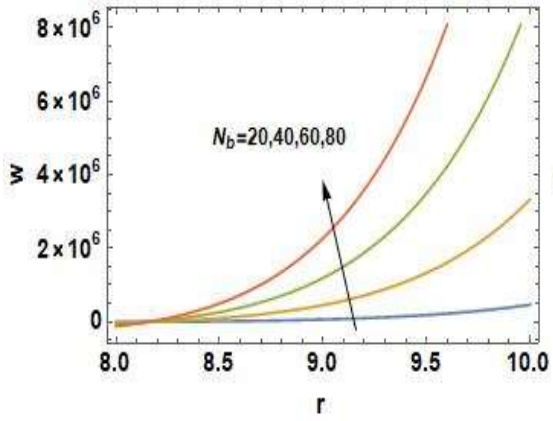

Fig. 22. The influence of r on w with N_b

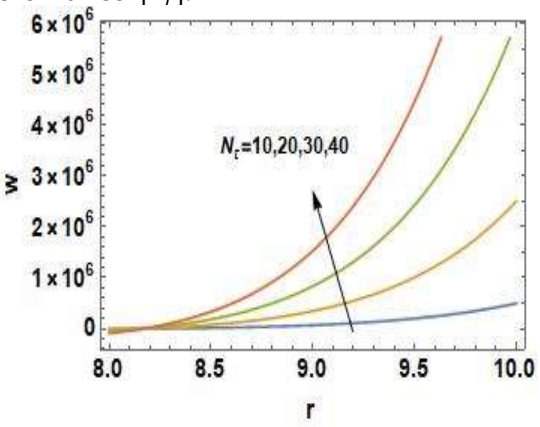

Fig. 23. The influence of r on w with N_t

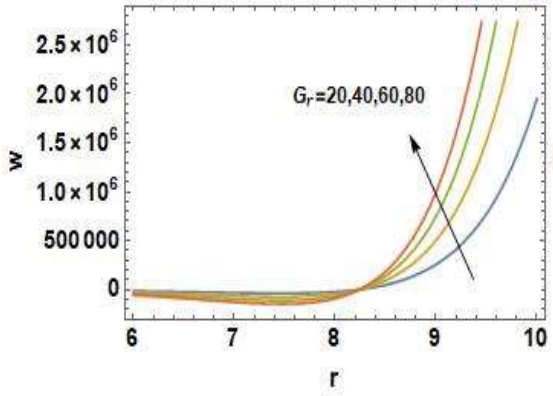

Fig. 24. The influence of r on w with G_r

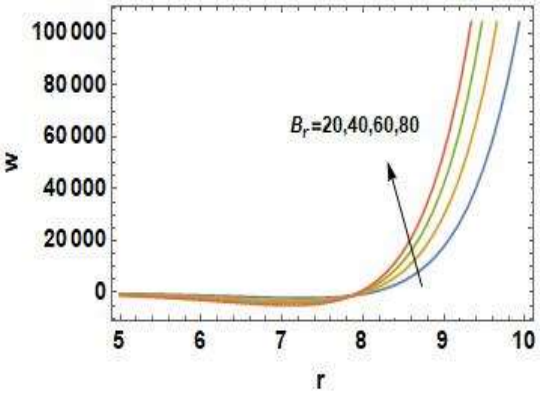

Fig. 25. The influence of r on with B_r

CONCLUSIONS

To calculate the impacts of numerous physical characteristics on volume flow rate, the Rubinow and Keller & Mazumdar methods are utilised. The phenomenon of entrapment is visually demonstrated. Here are the main points to consider

1. The flux along the radius is investigated for various values of $t_1, t_2, K, A, N_b, N_t, G_r, m$ and N. The flux of a micropolar fluid in an elastic tube through peristalsis rises as $t_1, t_2, K, A, N_b, N_t, G_r, m$ and N increase.
2. The Volume Flux diminishes as the Local Nanoparticle Grashof number (B_r) grows.
3. The trapping boluses grow as the values of N_b and $B_r$increase, while the trapping boluses decrease when the values of N_t and G_r increase.
4. The Velocity profile rises as N_b, N_t, G_r and B_r rise.

REFERENCES

1. Latham TW, fluid motion in a peristaltic pump, MS. Thesis, Massachusetts Institute of Technology, Cambridge (1996).
2. Maruthi Prasad K, Ramana Murthy JV, VK Narla. Unsteady Peristaltic Transport in Curved Channels. *Physics of Fluids, DOI:10.1063/1.4821355, 25 (2013) 091903.*
3. Maruthi Prasad. K, Subadra. N, Srinivas. M. A. S, Study of Peristaltic Motion of Nanoparticles of a Micropolar Fluid with Heat and Mass Transfer Effect in an Inclined Tube. *International Conference on Computational Heat and Mass Transfer, 127, 694-702, 2015*.
4. B.B. Divya, G. Manjunatha, C. Rajashekar, Hanumesh Vaidya, K.V. Prasad. Impact of Variable Liquid Properties on Peristaltic Mechanism of Convectively Heated Jeffrey Fluid in a Slippery Elastic Tube. *12(15), 2151-8629, 2019.*
5. R. Ravikumar, G. Arul Freeda Vinodhini, J. Prakash, Heat Transfer and Slip Effects on the MHD Peristaltic Flow of Viscous Fluid in a Tapered Microvessels: Application of Blood Flow Research, *International Journal of Engineering and Advanced Technology (IJEAT), 9(1), 2249 – 8958, 2019.*
6. Gudekote, M. ., & Choudhari, R., Slip Effects on Peristaltic Transport of Casson Fluid in an Inclined Elastic Tube with Porous Walls, *Journal of Advanced Research in Fluid Mechanics and Thermal Sciences, 43(1), 67–80, 2020*.
7. Choi SUS. Enhancing Thermal Conductivity of Fluids with Nanoparticles, In Signer DA, Wang HP (eds) Developments and applications of Non-Newtonian flows. *ASME, New York, 66, 99-105, 1995.*
8. Noreen Sher Akbar and S.Nadeem . Peristaltic Flow of a Micropolar Fluid with Nanoparticles in Small Intestine. *Applied Nanoscience, 3(6), 461-468. 2013.*
9. K. Maruthi Prasad, N. Subadra, M. A. S. Srinivas. Peristaltic Transport of a Nanofluid in an Inclined Tube. *American Journal of Computational and Applied Mathematics, 5(4), 117-128, 2015*
10. C. Haseena, A. N. S. Srinivas, C. K. Selvi, S. Sreenadh, and B. Sumalatha, The Influence of elasticity on Peristaltic Flow of Nanofluid in a Tube, *American Scientific Publishers, 10, 590-599, 2021.*

A. M. Abd-Alla, Esraa N.Thabet, F.S. Bayones, Numerical Solution for MHD Peristaltic Transport in an Inclined Nanofluid Symmetric Channel with Porous medium, *Scientific reports, 12, 3348, 2022.*

11. Maruthi Prasad. K, Subadra. N, Srinivas. M. A. S, Study of Peristaltic Motion of Nanoparticles of a Micropolar Fluid with Heat and Mass Transfer Effect in an Inclined Tube. *International Conference on Computational Heat and Mass Transfer, 127, 694-702, 2015*.
12. C.K. Selvi, A.N.S. Srinivas. Peristaltic Transport of Herschel-Bulkley Fluid in a Non-Uniform Elastic Tube. *8(3), 253-262, 2018.*
13. Ajaz Ahmad Dar, Peristaltic Motion of Micropolar Fluid with Slip Velocity in a Tapered Asymmetric Channel in Presence of Inclined Magnetic Field and Thermal Radiation. *Sohag J. Math. 8(1), 9-22, 2021*.
14. Prasad, K. M. and Yasa, P. R., Micropolar Fluid in Tapering Stenosed Arteries having Permeable Walls. *Malaysian Journal of Mathematical Sciences, 15(1), 157-171, 2021*.
15. C. K. Selvi, A. N. S. Srinivas. The Effect of Elasticity on Bingham Fluid Flow in a Tube. *Int. journal of Mechanical Engineering and Technology, 8(8), 554-564, 2017.*
16. B. Sumalatha and S. Sreenadh, Poiseuille flow of a Jeffrey Fluid in an Inclined Elastic Tube. *Int. journal of Eng. Sciences & Research Technology, 7(1), 150-160, 2018.*
17. C.K. Selvi, A. N. S. Srinivas and S. Sreenadh. Peristaltic Transport of a Power-Law Fluid in an Elastic Tube. *Journal of Taibah University for Science, 12(5), 687-698, 2018.*
18. C. Haseena, A. N. S. Srinivas, C. K. Selvi, S. Sreenadh, and B. Sumalatha, *The Influence of elasticity on Peristaltic Flow of Nanofluid in a Tube, American Scientific Publishers, 10, 590-599, 2021.*
19. He JH. Homotopy Perturbation Technique. *Computer Methods in Applied Mechanics and Engineering. 178(3-4), 257-262, 1999.*
20. Mazumdar, N.J. Biofluid Mechanics, World Scientific, Chapter.5, Singapore. 1992.
21. S. I. Rubinow, Joseph B. Keller. Flow of a Viscous Fluid through an Elastic Tube with Applications to Blood Flow. *J. theor. Biol. 35(2), 299-313, 1972.*